

Thomas Wendl\*, Brigitte Wendl and Peter Proff

# An analysis of initial force and moment delivery of different aligner materials

<https://doi.org/10.1515/bmt-2025-0003>

Received January 6, 2025; accepted February 17, 2025;

published online March 3, 2025

## Abstract

**Objectives:** The aim of this study was to clarify the applied initial forces and moments by different aligners of various materials and manufacturing methods.

**Methods:** The finite-element-method was used to analyze the forces and moments generated by the aligners on a maloccluded tooth. Plaster models of dental arches with a mesiorotated tooth 11 were fabricated, digitized and virtually analyzed. Four types of aligners with various layer thicknesses were selected: two splints with novel shape memory properties: a printable aligner made of the resin Tera Harz TC-85 DAC (Graphy Inc., South Korea) and a self-manufactured aligner consisting of the components polypropylene carbonate and thermoplastic polyurethane. The other two aligners were conventional, thermoformable aligners: CA® Pro Clear Aligner (Scheu Dental GmbH, Germany) and Erkodur-al (Erkodent Erich Kopp GmbH, Germany).

**Results:** The force and moment analyses showed that the thermoformable CA® Pro Clear Aligner exhibited the highest values. The thermoformed Erkodur-al aligner showed the lowest force loads for all layer thicknesses. The Graphy printed splint showed similar results compared to Erkodur-al at layer thicknesses of 0.40 mm and 0.50 mm.

**Conclusions:** To avoid periodontal overloading, aligners with lower force and moment delivery should be chosen for this type of tooth movement.

**Keywords:** shape-memory; force; moment; single-multi-layer; aligner; finite-element-method

## Introduction

Orthodontic tooth movement occurs because of compressive and tensile forces. Bone resorption transpire on the pressure side of a tooth. On the opposite side, traction on the periodontal fibers causes bone growth. There are various options for applying the necessary forces to the teeth – removable (e.g., plates, aligners) and fixed (bands and brackets) appliances [1].

The development and use of aligners has become increasingly important with the advancement of material technology and the growing desire of patients for appliances that are as inconspicuous and aesthetically pleasing as possible. Currently, the orthodontic treatment results with aligners are limited for certain tooth movements. The assessment of the orthodontic forces of transparent aligners with their complex biomechanical properties is primarily based on clinical experience [2].

The force exerted by aligners differs from other orthodontic appliances. The elastic restoring forces of the material ensure the tooth movement, while at the same time enabling immediate retention of the teeth. The material must have a certain rigidity to exert sufficient force, have an elastic restoring capacity and should be able to move and hold the tooth through its undercuts [3].

Aligners are made from various polymers, such as polyethylene terephthalate glycol (PETG) and polyurethane [4]. They can achieve good results in mild to moderate treatment cases in a short period of time [5]. However, aligners are more limited in their use for extensive tooth realignments [6]. For this reason, improvements in the aligner materials regarding their force and moment exertion are important.

The so-called “smart materials” represent a new group of materials. One subgroup are smart polymers, which include shape memory polymers (=SMPs). They are characterized by a shape memory effect (=SME) and thus have the ability to change their macroscopic shape in response to a corresponding stimulus (e.g. temperature) and retain this temporary shape. Reactivation by means of an external stimulus restores the SMPs to their original (=permanent) shape. The shape memory behavior of physically cross-linked, amorphous polymers is primarily influenced by the glass transition temperature  $T_g$  of the soft segment areas.  $T_g$  is the temperature above which the elasticity of a polymer decreases and a previously stiff polymer exhibits rubber-like

\*Corresponding author: Thomas Wendl, Department of Orthodontics, University of Regensburg, Regensburg, Germany, E-mail: thomas.wendl92@gmail.com

Brigitte Wendl, Department of Orthodontics, Medical University Graz, Graz, Austria, E-mail: brigitte.wendl@medunigraz.at

Peter Proff, Department of Orthodontics, University of Regensburg, Regensburg, Germany, E-mail: peter.proff@ukr.de

behavior. SMPs can therefore switch reversibly between a permanent and temporary form. SMPs have good formability and are characterized by low costs, simple production, biocompatibility and customizable programming with adaptable physical properties [7]. With the help of these shape memory restoration forces, it could be shown that the use of a shape memory aligner can replace the application of three consecutive conventional aligners [8]. This makes it possible to reduce the number of aligners used per treatment. In addition, resin consumption is reduced and overall costs are lowered.

However, it is essential to thoroughly investigate the mechanical behavior of the SMP aligners compared to conventional aligners. The forces and moments emitted by the shape memory recovery must be measured and compared to the forces that occur in conventional tooth movement splints. Although there are several patents, there is still a lack of research and publications that examine these smart polymers in relation to orthodontic applications [9].

For a finite-element-simulation of orthodontic forces of aligners, the material parameters for each component of the model must be specified correctly [10]. To simplify the model, the linear-elastic mode can be used [11]. In the literature large deviations of Young's modulus of enamel are described [10, 12]. More recent studies define a value of 80 GPa [13, 14]. This is similar to the elastic modulus of the plaster models. The stated Young's modulus of conventional aligners is in the range of 0.5–2.2 GPa [15, 16].

## Materials and methods

The following aligners were selected for the analysis of the force and moment delivery to correct the mesiorotated tooth 11:

- CA® Pro Clear Aligner (Scheu Dental GmbH, Germany) =three-layer foil made of a copolyester double-shell construction and a thermoplastic elastomer core. It is a thermoforming splint.
- Erkodur-al (Erkodent Erich Kopp GmbH, Germany) =copolyester (CAS no.: 261716-943). This is a thermoforming splint.
- SMP aligner, which was produced in a previous cooperation with the University of Leoben and consists of the components PPC (=polypropylene carbonate) and TPU (=thermoplastic polyurethane) and has shape memory properties. It is a thermoforming splint.
- Tera resin TC-85 (Graphy Inc., South Korea) =direct 3D printed aligner with shape memory properties, consisting of a vinyl ester urethane material

Figure 1 shows the mesiorotation of tooth 11 on the digital model of the maxilla.

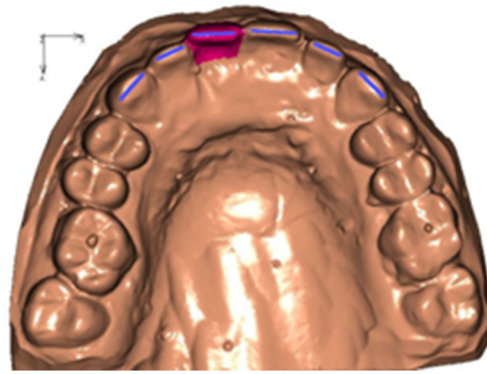


**Figure 1:** Digital dental arch with malpositioned incisor 11, with axes.

## Fabrication of set-up models, malocclusion models and drilling templates

A plaster model (Ernst Hinrichs GmbH, Germany) was fabricated with the actual situation of a clinical patient (=malocclusion model), in which the upper central incisor is mesiorotated by 10°. This tooth 11 was then manually separated from the dental arch of the plaster model using a plaster cutter, brought into an ideal tooth position on the dental arch and fixed with a pink-colored wax (Beauty Pink, Integra Miltex GmbH, Germany). This set-up model was duplicated and four further plaster models with the corrected position of the tooth 11 were fabricated. In order to be able to ensure an exact digital assignment of the splints and models later on, fine interdental/gingival holes were drilled on the set-up models in the premolar region, palatally at the level of the third palatal rugae and occlusally in the molars 16 and 26, as there is no tooth movement at these points. Consequently, a type of drilling template could be fabricated in order to transfer the drill holes to the thermoformed or printed aligners and thus also to the malocclusion models. This was followed by scanning the malocclusion models and the models with the improved position of tooth 11.

Figure 2 shows a malocclusion model with drill holes as well as the drilling template.

## Fabrication of the aligners using the thermoforming process and the direct printing process

The next step was thermoforming and printing the splints according to the set-up model. The thermoforming of the splints was carried out using the Ministar thermoforming unit (Scheu Dental GmbH, Germany) in accordance with the manufacturer's instructions.



**Figure 2:** Drilled holes on the malocclusion model by using a drilling template.

The so-called Graphy aligners, which are made of TC-85 DAC Tera Harz (Graphy Inc., South Korea), were printed after the digital planning step (planning software UNIZ Dental, UNIZ, United States of America) using the 3D printer UNIZ NBee (UNIZ, United States of America). After the printing process, the splints were in a soft condition and they were removed from the printing platform with their support structures. This was followed by placing the aligners in a centrifuge (Tera Harz spinner, Graphy Inc., South Korea). Due to the shape memory properties of the aligners, the deformation of the aligners during the manufacturing process had no negative effects. After the support structures have been removed, the aligners were UV light-cured under nitrogen oxide (Tera Harz Cure 2, Graphy Inc., South Korea). This process changed the color of the aligners from slightly yellowish to a clear colorless appearance. The additional effect of the Tera Harz TC-85 DAC material is the shape memory effect. Before being transferred to the model, the Graphy splint was heated with hot water for a softening effect. In this condition, the aligner could be placed on the model easier. Afterwards it returned to its original shape and exerts the corresponding force. In addition, any residual monomers could be removed.

The holes in the plaster models were transferred to the aligners. After processing, the splints, which were still on the model, were scanned. The aligners were then removed from the models and scanned from the inside and outside, using the scanning spray (Zirko Scanspray, Zirkonzahn S.R.L., Italy). The arrangement of the scans was standardized, i.e., always aligned in the same way. The generated digital models of the dental arches and aligners were exported as STL files in the processing and editing software MeshLab (ISTI-CNR, Italy). All scans were performed with the MedIT i500 3D scanner (MedIT, South Korea).

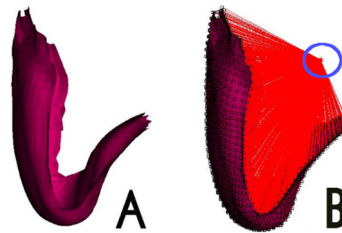


**Figure 3:** Misaligned tooth in side view. A: surface, B: connection to evaluation node.

### Development of a suitable finite-element-model for force determination

In order to determine the forces acting on the misaligned tooth, the entire surface (=the nodes of the surface discretization) was rigidly coupled to a central node. This means that forces and moments acting on the surface can be evaluated at this point and shifted in space as required by calculation. Figure 3A shows the surface of the misplaced tooth, which is loaded by the aligner during the simulation. Figure 3B shows the same tooth with a rigid connection to the central evaluation node (in blue).

The geometry of the malocclusion model and the different splints was captured using a scanner and saved as a triangulated model (stl-file format). It is important to note that the recorded geometries only characterize the surface, not the volume.

For this reason, the geometry was adapted by remeshing the basic models consisting of triangles. The geometry remained preserved, but the many triangles were largely replaced by quadrilaterals. This made it essentially easier to perform the calculation and reduced the number of degrees of freedom (i.e. the nodes at which the forces and displacements were calculated). The average element edge length of approximately 0.25 mm was selected so that the geometry had the best possible resolution and at the same time the calculation time was kept within certain limits.

The malocclusion model was restricted to the relevant areas, and the splints were also trimmed to the regular application size.

The adjustment of the aligner position (position in three spatial directions, angle around the three spatial axes) posed a greater challenge. This position could not be definitively defined and the aim was to completely eliminate the constraints once the splint was in place. In this state, the splint was free of external forces and the reality could best be described.

As described, the misaligned tooth was considered to be separate from the rest of the geometry and the forces and moments acting on it were analyzed individually. This assumption is graphically illustrated in Figure 3 and was

used for all calculations. From a simulation point of view, the application of the splint required the use of a special system consisting of the following steps:

a. Thermal expansion – “heating the splint”

A specific coefficient of thermal expansion is added to the material model for the dental splints. This allows the splint to be expanded by applying a thermal load. In this phase, the contact formulation is switched off and the interpenetrating surface sections can move relative to each other without hindrance.

This effect can be used to expand the splint. The aim was to ensure that there was no overlap with the dental arch after applying the thermal expansion.

b. Preventing stability effects

The thermal boundary conditions induce membrane stresses, which – as the calculation is generally non-linear – lead to stability problems (shell buckling). In the simulations, such effects, wherever they occurred, had to be prevented by additional boundary conditions.

c. Thermal expansion – cooling of the aligner

To apply the splint to the dental arch, the contact formulation is activated (prevention of penetration) and the splint is gradually cooled down again. This creates a condition in which the splint is in contact with the dental arch.

d. Relaxation of the constraints

The calculation requires the existence of equilibrium states. During the warm-up and cool-down phases, these states had to be ensured by suitable boundary conditions. At the end, the splint had to hold on to the dental arch on its own and this state requires the complete removal of all constraints.

e. Evaluation of the load data

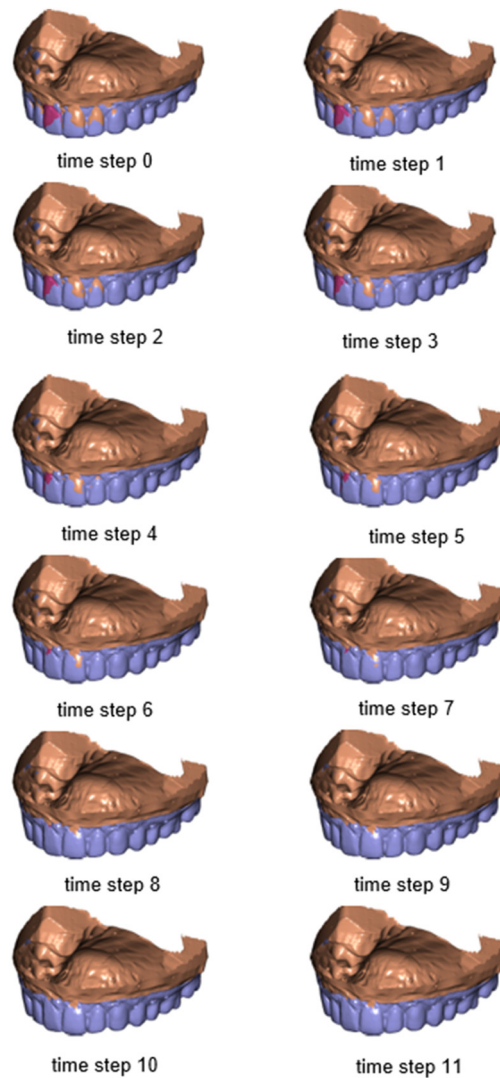
The calculation is evaluated by determining the forces and moments on the defined central node, which comprises the force effect of the aligner on the misaligned tooth in its entirety.

Figure 4 shows the time steps in which the thermal boundary condition is applied to the splint, as well as the aligner fully applied to the arch.

## Basic assumptions for the finite-element-calculation

The study is based on the following basic assumptions:

a. Stiff dental arch



**Figure 4:** Stretching and complete positioning of the aligner from time step 0 to time step 11.

The dental arch and all its surrounding structures were assumed to be immobile. This corresponds to a conservative approach, as the real mobility of the teeth under the effect of the force reduces the simulated forces. The results can therefore be regarded as a kind of limitation for the forces that actually occur.

b. Linear-elastic material model

The splint material was considered using a linear elastic material model due to the comparatively low strains. The implementation of a non-linear material model would require extensive measurement of the material and the separate production of sample geometries.

c. Definition of the moduli of elasticity



In the investigations, the modulus of elasticity of the different tooth adjustment splints was varied according to the manufacturer's specifications or publications.

#### d. Contact

The contact of the splints with the dental arch was considered using non-linear surface-to-surface contact. A coefficient of friction of 0.001 was used. This can be explained by the fact that the frictional forces are quickly reduced after the real splint is applied and a state of almost frictionless contact is achieved relatively rapidly.

#### e. Shell model

The aligner geometry was considered as a shell geometry according to the concept of structural elements. The thickness was specified as a constant and varied in different calculations. This does not fully correspond to reality, as the thicknesses vary depending on the manufacturing process. However, it was possible to specify a force range in which the force is very likely to be located.

The thickness grading was carried out considering the thicknesses that actually occurred in the model. Three thicknesses were therefore calculated to allow interpolation between these thicknesses and, up to certain limits, extrapolation. In addition, the results of the thickest splints can also be used as a limit for the force effect.

Statistical analyses were performed using IBM SPSS Statistics® Ver. 23 (IBM, Armonk, NY, USA).

## Results

### Exemplary force calculation

For the SMP aligner with a thickness of 0.4 mm, the evaluation of the force and moment reactions for tooth 11 is shown in Figure 5.

The following individual phases of the calculation can be distinguished:

- $t \in [0, 1]$ : Warm-up phase

No force is transferred to the tooth.

- $t \in [1, 2]$ : Cooling phase

The aligner is placed on the dental arch. A force is applied during the cooling process.

- $t \in [2, 3]$ : Relaxation phase

During this phase, the final constraints are relaxed. At the end, the splint rests on the dental arch on its own. These final forces and moments are acting on the misaligned tooth.

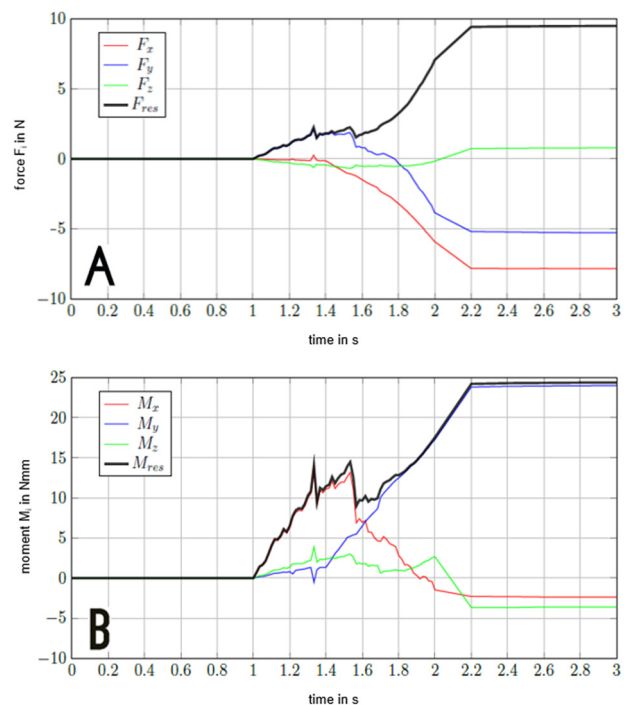


**Figure 5:** Resulting force (A) and moment (B) reactions generated by the SMP aligner on the tooth 11 measured at the central node.

Table 1 describes the force and moment loads at the central node for the different aligners.  $F_{res}$  and  $M_{res}$  represent the forces and moments, which result from the sums of the forces and moments acting in all three spatial directions.

Figure 6 shows the respective force and moment values ( $F_{res}$  and  $M_{res}$ ) of the individual aligners.

The thermoformed CA® Pro Clear Aligner showed the highest values for all three examined splint thicknesses (0.4 mm, 0.5 mm and 0.6 mm) regarding the resulting force and moment loads. In contrast, the Erkodur-al aligner demonstrated the lowest force loads for the layer thicknesses 0.4 mm, 0.5 mm and 0.6 mm. The direct printed Graphy splint presented similar results in terms of force application compared to Erkodur-al at layer thickness of 0.4 mm. Regarding the delivered moments the Graphy aligner generated the lowest values at the at layer thicknesses of 0.4 mm and 0.5 mm.

The force values of the CA® Pro Clear Aligner were statistically significantly greater than the force values of Erkodur-al ( $p$ -value=0.006) and Graphy ( $p$ -value=0.016).

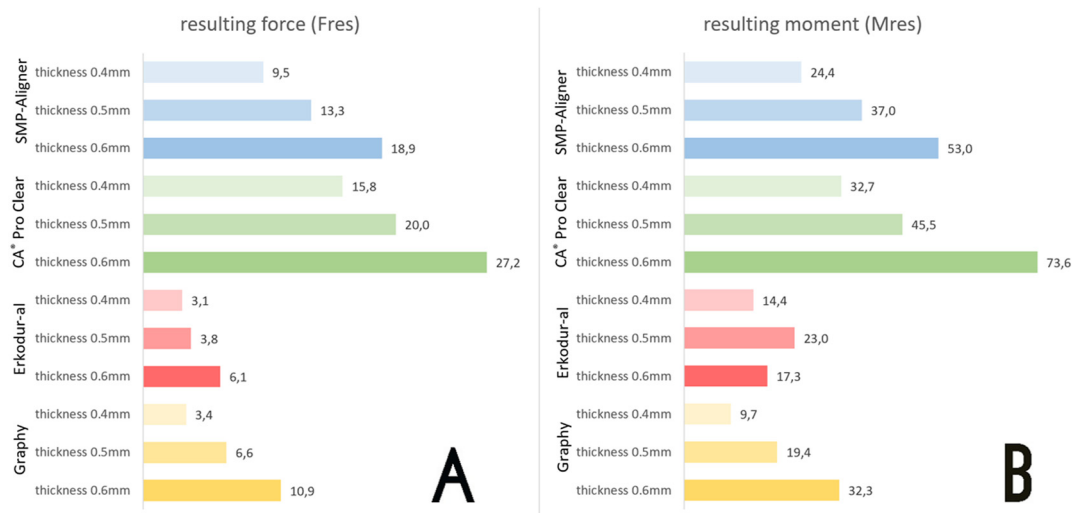
Figure 7 shows the contact status between the dental arch and the aligner. The greatest forces are effective at the points shown in red.

## Discussion

Excessive force on the teeth during orthodontic treatment can lead to root resorption or even tooth loss [17]. Therefore,

**Table 1:** Force and moment loads at the central node.

	Thickness	$F_x$	$F_y$	$F_z$	$F_{res}$	$M_x$	$M_y$	$M_z$	$M_{res}$
SMP aligner	0.40 mm	-7.8	-5.3	0.79	<b>9.5</b>	-2.4	24.0	-3.7	<b>24.4</b>
	0.50 mm	-11.5	-6.6	1.0	<b>13.3</b>	-1.7	36.4	-6.5	<b>37.0</b>
	0.60 mm	-15.9	-10.1	1.6	<b>18.9</b>	-3.3	52.6	-6.9	<b>53.0</b>
CA® pro clear aligner	0.40 mm	-10.8	-11.8	0.9	<b>15.8</b>	-11.5	30.6	-2.3	<b>32.7</b>
	0.50 mm	-15.0	-13.2	0.8	<b>20.0</b>	-3.2	45.4	0.5	<b>45.5</b>
	0.60 mm	-22.4	-15.4	0.9	<b>27.2</b>	-4.2	72.8	-9.6	<b>73.6</b>
Erkodur-al	0.40 mm	0.6	-3.1	-0.1	<b>3.1</b>	7.0	-5.2	11.4	<b>14.4</b>
	0.50 mm	1.4	-3.5	-0.3	<b>3.8</b>	12.4	-9.7	16.8	<b>23.0</b>
	0.60 mm	1.0	-6.0	-0.6	<b>6.1</b>	10.7	-1.4	13.5	<b>17.3</b>
Graphy	0.40 mm	-2.8	-1.8	0.1	<b>3.4</b>	-5.1	8.2	-0.4	<b>9.7</b>
	0.50 mm	-5.0	-4.4	0	<b>6.6</b>	-12.1	14.6	3.9	<b>19.4</b>
	0.60 mm	-8.4	-6.9	-0.6	<b>10.9</b>	-19.8	25.1	4.6	<b>32.3</b>

**Figure 6:** Resulting forces (A) and moments (B) at the central node.**Figure 7:** Contact status on the dental arch.

an optimal external force system is the key to a successful orthodontic treatment [18]. Due to the lack of suitable instruments to quantify the orthodontic force, the predictability of treatment with aligners for specific tooth movements is low in many cases [19, 20]. Therefore, the final treatment result can deviate by up to 50 % from the expected

result, which limits the clinical use of aligners [21, 22]. Hence, accurate measurement and understanding of the forces and moments exerted by aligners are crucial for the development of a well-founded orthodontic treatment plan.

For this reason, this work aims to contribute to a better understanding of the mechanics of orthodontic aligners by designing a suitable finite-element-model. Since the dental arch and splint were always scanned separately, it was difficult to align the two geometries with each other. Although the aligners could be optically orientated, the initial position influenced the force situation at the end of the cooling phase. During the relaxation, larger external loads had to be removed in some cases. Convergence problems could occur in this phase. Thus, the orientation of the splint played a decisive role in the calculation behavior (especially in the last phase). Markings, in the form of drilled holes, were made both on the models and on the splints to

facilitate their superimposition. The so-called “heating” method was proved to be suitable, although stability problems arose using the thin splint thicknesses.

This approach is able to calculate the effect of digitized splints on scanned dental arches in a realistic way. Since the aligners were modeled as a shell, a simple change in thickness is usually possible if a computable model is available. This made it possible to realistically limit the force effect on the misaligned teeth.

Thermoformed aligners made of PET-G are still associated with high rigidity in the standard 0.5 mm thin version. It is therefore assumed that even with this layer thickness, the recommended forces for tooth movement are likely to be significantly exceeded. Therefore, a reduction in tooth movement per setup step (this is associated with increased laboratory work due to an increase in treatment steps) or even thinner aligners than 0.5 mm layer thickness should be used. This would lead to a reduction in force and rigidity and possible side effects can be avoided [23].

In finite-element-simulations, the shape of the meshing and the selection of the appropriate element class play a decisive role in ensuring sufficient quality and accuracy of the numerical analysis. Determining the contact parameters between the aligner and the teeth is difficult due to the individual shape of the aligners. Therefore, the friction between the aligner and the teeth was neglected in relation to the existence of dissimilarity between the aligner material and the tooth [10, 24]. In addition, the thicker the material of the aligner, the higher the forces generated [23, 25]. Clinical findings show that the risk of root resorption is lower when using aligners with reduced thickness [26].

For simplification, a linear-elastic model was assumed. In addition, although the test setups are rigid, there is still a certain flexibility of the devices, which is not considered in the mathematical FE-model. All these points mentioned can cause differences in the measurement.

Nevertheless, the resulting forces are still higher than the ideal orthodontic force for physical movements, which is between 0.75 N and 1.25 N [27]. Rotation describes the rotation of the tooth around its longitudinal axis and the rotation of the longitudinal axis around a center of rotation. According to Reitan, a force of 0.2–0.75 N, depending on the tooth, is specified to perform this movement [28]. In the literature, moments of 35.3–71.8 Nmm are described for the rotational movement [25, 29]. This is consistent with the evaluations in this study. However, it should be noted that Hahn et al. only examined thermoformed aligners with a thickness of 0.5 mm, 0.625 mm and 0.75 mm, which extended 2–4 mm above the gingival margin [25]. Elkholy et al. also investigated the forces and moments acting on a

mandibular incisor during rotational movement. In this study, thermoformed aligners with thicknesses of 0.3 mm, 0.4 mm, 0.5 mm, 0.625 and 0.75 mm were examined. The forces and moments were recorded using a sensor. The results for the moments were between 17.48 Nmm and 91.58 Nmm. The applied forces were in the range between 3.65 N and 19.70 N [26]. This also shows a good agreement with the present work.

Furthermore, studies demonstrate that the initial forces exerted by aligners exceed the recommended values for orthodontic movements by a factor of six. Further studies also present that the forces and moments transmitted from the aligner to the tooth decrease over time [30, 31].

Low moments should be applied to the periodontium to avoid its damage. In the study by Elkholy et al., a maximum derotation of 10° per set-up step was specified, resulting in a derotation moment of 15 Nmm [32]. Furthermore, this research group determined similar values regarding the force and moment load of thermoformed aligners compared to this work. The results of the analysis by Seo et al. demonstrate that orthodontic treatment with aligner of 0.75 mm thickness resulted in up to 6 % higher stresses in the periodontal ligament compared to treatment with a 0.50 mm thick aligner [33]. This study also showed that higher aligner thicknesses are associated with greater force and moment loads.

Although the results of the present work are promising, this study can only be regarded as a proof of concept, as it is an *in vitro* study. In addition, there is hardly any biomechanical reference data regarding rotational movements. Furthermore, bone modeling due to orthodontic forces is a complicated biological process resulting from a complex biomechanical reaction of the periodontal tissues [34].

Depending on the degree of malocclusion, an average of 30 to 60 aligners must be fabricated to correct the malocclusion over a period of several months. The ability of the newly developed polymer with shape memory effect has the potential to reduce the number of steps required during the orthodontic treatment compared to the use of conventional aligner materials [8]. Regarding the efficiency of individual tooth movements, it was shown that rotational movements with aligners can be considered less predictable [35].

Modifications of the developed model could be made in future studies. This can be done by adding further parameters, for example the periodontal ligament and the alveolar bone. An additional extension of this model would be intermediate steps or new set-up situations to determine the force more precisely over a certain time span, because the initial forces and moments generally decrease after a certain period of time during treatment. It would thus be beneficial to create a finite-element-model for future studies that can

measure force and moment loads after specified time intervals. However, further modifications of the model would lead to increased complexity of the calculations. In general, it should also be noted that a serial or industrial application is not possible with this methodology due to the long calculation time with a large number of iterations.

## Conclusions

Treating malocclusions with aligners can initially lead to high forces and moments. Depending on the material and thickness of aligners these values may vary considerably. With an aligner thickness of 0.4 mm, the force delivery was between 3.1 N and 15.8 N and occurring moments were between 9.7 Nmm and 32.7 Nmm. Higher values for both the forces and the moments were observed with thicker aligners.

To avoid overloading periodontal structures, low forces and rotational moments should be applied on a tooth. This must be considered when selecting the aligner material with the appropriate layer thickness. Thus, thinner aligners should be used. Future experimental and clinical studies with different aligner modifications and attachment geometries could help to optimize the derotation effect of aligners and minimize the collateral force and moment components. The shape memory effect programmed into certain aligners could contribute, as this effect makes it possible to exert constant gentle forces over a longer period of time and consequently avoid larger initial forces.

The finite-element-method is a promising approach that can lead to a better understanding of the mechanical behavior of orthodontic aligners. The current model has limitations regarding the parameters used. In this study, all calculation problems could be eliminated.

**Acknowledgments:** In memoriam. Wolfgang Kern, former chairholder in chemistry of polymeric materials, Montanuniversität Leoben, Austria, who helped to develop a smart material with shape-memory properties.

**Research ethics:** Not applicable.

**Informed consent:** Not applicable.

**Author contributions:** All authors have accepted responsibility for the entire content of this manuscript and approved its submission.

**Use of Large Language Models, AI and Machine Learning Tools:** None declared.

**Conflict of interest:** The authors state no conflict of interest.

**Research funding:** None declared.

**Data availability:** Not applicable.

## References

1. Choy K. Burstone's biomechanical foundation of clinical orthodontics. 2. Auflage. Batavia: Quintessenz; 2022:516 p.
2. Zeng J, Zhang Z, He X, Yuan H, Li Y, Song M. Real-time GNSS multiple cycle slip detection and repair based on a controllable geometry-based method in relative positioning. *Meas (Lond)* 2023;216. <https://doi.org/10.1016/j.measurement.2023.112940>.
3. Graf S. Direkt gedruckte aligner – der heilige gral in der kieferorthopädie? *Inf Orthod Kieferorthop* 2023;55:18–22.
4. Ercoli F, Tepedino M, Parziale V, Luzi C. A comparative study of two different clear aligner systems. *Prog Orthod* 2014;15:31.
5. Simon M, Keilig L, Schwarze J, Jung BA, Bourauel C. Forces and moments generated by removable thermoplastic aligners: incisor torque, premolar derotation, and molar distalization. *Am J Orthod Dentofacial Orthop* 2014;145:728–36.
6. Simon M, Keilig L, Schwarze J, Jung BA, Bourauel C. Treatment outcome and efficacy of an aligner technique—regarding incisor torque, premolar derotation and molar distalization. *BMC Oral Health* 2014;14:18.
7. Wendl T, Bandl C, Kern W, Wendl B, Proff P. A new method for successful indirect bonding in relation to bond strength. *Biomed Eng-Biomed Te* 2022;67:403–10.
8. Elshazly TM, Keilig L, Alkabani Y, Ghoneima A, Abuzayda M, Talaat S, et al. Primary evaluation of shape recovery of orthodontic aligners fabricated from shape memory polymer (a typodont study). *Dent J* 2021;9:31.
9. Bruni A, Serra FG, Deregibus A, Castroflorio T. Shape-memory polymers in dentistry: systematic review and patent landscape report. *Materials* 2014;12:2216.
10. Barone S, Paoli A, Razionale AV, Savignano R. Computer aided modelling to simulate the biomechanical behaviour of customised orthodontic removable appliances. *Int J Interact Des Manuf* 2016;10:387–400.
11. Mascarenhas R, Shenoy S, Parveen S, Chatra L, Husain A. Evaluation of lingual orthodontic appliances. *J Comput Methods Sci Eng* 2017;17:253–60.
12. Kettenbeil A, Reimann S, Reichert C, Keilig L, Jäger A, Bourauel C. Numerical simulation and biomechanical analysis of an orthodontically treated periodontally damaged dentition. *J Orofac Orthop/Fortschr Kieferorthop* 2013;74:480–93.
13. Sadyrin E, Swain M, Mitrin B, Rzhepakovsky I, Nikolaev A, Irkha V, et al. Characterization of enamel and dentine about a white spot lesion: mechanical properties, mineral density, microstructure and molecular composition. *Nanomater* 2020;10. <https://doi.org/10.3390/nano10091889>.
14. Ausiello P, Dal Piva AM, Borges AL, Lanzotti A, Zamparini F, Epifania E, et al. Effect of shrinking and no shrinking dentine and enamel replacing materials in posterior restoration: a 3D-FEA study. *Appl Sci* 2021;11. <https://doi.org/10.3390/app11052215>.
15. Tamburrino F, D'Antò V, Bucci R, Alessandri-Bonetti G, Barone S, Razionale AV. Mechanical properties of thermoplastic polymers for aligner manufacturing: in vitro study. *Dent J* 2020;8. <https://doi.org/10.3390/dj8020047>.
16. Al-Joubori H, Hussein S, Kadhum S. Comparison of the hardness and elastic modulus of Different orthodontic aligners' materials. *Int J Pharma Sci Res* 2018;5:19–25.
17. Tobushi H, Hara H, Yamada E, Hayashi S. Thermomechanical properties in a thin film of shape memory polymer of polyurethane series. *Smart Mater Struct* 1996:483–91. <https://doi.org/10.1088/0964-1726/5/4/012>.



18. Liu L, He B, Zhuang J, Zhang L, Lv A. Force measurement system for invisalign based on thin film single force sensor. *Meas* 2017;97:1–7.
19. Huang H, Tang W, Tan Q, Yan B. Development and parameter identification of a visco-hyperelastic model for the periodontal ligament. *J Mech Behav Biomed Mater* 2017;68:210–5.
20. Schmidt F, Lapatki BG. Effect of variable periodontal ligament thickness and its non-linear material properties on the location of a tooth's centre of resistance. *J Biomech* 2019;94:211–8.
21. Ho CT, Huang YT, Chao CW, Huang TH, Kao CT. Effects of different aligner materials and attachments on orthodontic behavior. *J Dent Sci* 2021;16:1001–9.
22. Alansari RA, Faydhi DA, Ashour BS, Alsaggaf DH, Shuman MT, Ghoneim SH, et al. Adult perceptions of different orthodontic appliances. *Patient Prefer Adherence* 2019;13:2119–28.
23. Elkholy F, Panchaphongsaphak T, Kilic F, Schmidt F, Lapatki B. Forces and moments delivered by PET-G aligners to an upper central incisor for labial and palatal translation. *J Orofac Orthop* 2015;6:460–75.
24. Cai Y, Yang X, He B, Yao J. Finite element method analysis of the periodontal ligament in mandibular canine movement with transparent tooth correction treatment. *BMC Oral Health* 2015;15:106.
25. Hahn W, Engelke B, Jung K, Dathe H, Fialka-Fricke J, Kubein-Meesenburg D, et al. Initial forces and moments delivered by removable thermoplastic appliances during rotation of an upper central incisor. *Angle Orthod* 2010;80:239–46.
26. Elkholy F, Schmidt F, Jäger R, Lapatki BG. Forces and moments applied during derotation of a maxillary central incisor with thinner aligners: an in-vitro study. *Am. J. Orthod. Dentofac. Orthop* 2017;151:407–15.
27. Proffit W, Fields H, Larson B, Sarver D. *Contemporary orthodontics*, 6th ed. Philadelphia: Elsevier; 2018:744 p.
28. Reitan K. Clinical and histologic observations on tooth movement during and after orthodontic treatment. *Am J Orthod* 1967;10:721–45.
29. Iliadi A, Koletsi D, Eliades T. Forces and moments generated by aligner-type appliances for orthodontic tooth movement: a systematic review and meta-analysis. *Orthod Craniofac Res* 2019;22. <https://doi.org/10.1111/ocr.12333>.
30. Vardimon AD, Robbins D, Brosh T. In-vivo von mises strains during invisalign treatment. *Am. J. Orthod. Dentofac. Orthop.* 2010;138:399–409.
31. Kohda N, Iijima M, Muguruma T, Brantley WA, Ahluwalia KS, Mizoguchi I. Effects of mechanical properties of thermoplastic materials on the initial force of thermoplastic appliances. *Angle Orthod* 2012;83:476–83.
32. Elkholy F, Mikhael B, Schmidt F, Lapatki BG. Mechanical load exerted by PET-G aligners during mesial and distal derotation of a mandibular canine. *J Orofac Orthop/Fortschr Kieferorthop* 2017;78:361–70.
33. Seo JH, Eghan-Acquah E, Kim MS, Lee JH, Jeong YH, Jung TG, et al. Comparative analysis of stress in the periodontal ligament and center of rotation in the tooth after orthodontic treatment depending on clear aligner thickness – finite element analysis study. *Materials* 2021;14. Available from: <https://www.mdpi.com/1996-1944/14/2/324>.
34. Bourauel C, Freudenreich D, Vollmer D, Kobe D, Drescher D. Simulation of orthodontic tooth movements. *J Orofac Orthop* 1999;60:136–51.
35. Rossini G, Parrini S, Castrolforio T, Deregibus A, Debernardi CL. Efficacy of clear aligners in controlling orthodontic tooth movement: a systematic review. *Angle Orthod* 2015;85:881–9.